

SYNTHESIS AND PROPERTIES  
OF INORGANIC COMPOUNDSPhotocatalytic Activity of Titania Nanopowders Prepared  
by a Sol–Gel Process at Various pHsA. V. Agafonov<sup>a, b</sup>, A. A. Redozubov<sup>a</sup>, V. V. Kozik<sup>b</sup>, and A. S. Kraev<sup>a</sup><sup>a</sup>Institute of Solution Chemistry, Russian Academy of Sciences, ul. Akademicheskaya 1, Ivanovo, 153045 Russia<sup>b</sup>National Research Tomsk University, pr. Lenina 36, Tomsk, 634050 Russiae-mail: [ava@isc-ras.ru](mailto:ava@isc-ras.ru)

Received February 25, 2015

**Abstract**—A strategy has been proposed to prepare photocatalytically active titania nanopowders through a sol–gel route using high-degree molecular separation upon the dilution of reagents, high water/alkoxide ratios, high reagent mixing rates, and pH effects. This strategy has been successfully used to isolate, from sols, anatase powders with high surface areas (100–310 m<sup>2</sup>/g) dependent on the pH value during the synthesis. The photocatalytic activity of titania nanopowders prepared by the sol–gel process at various pHs has been tested in photodestruction of organic dyes (Rhodamine B, Methylene Blue, and Anthraquinone AcidBlue) in acid solutions. UV-radiation-induced dye destruction rates are found to depend on the surface properties (including surface area and  $\zeta$  potential) and hydration specifics of the titania.

DOI: 10.1134/S0036023615080021

The influence of various factors on the photocatalytic activity of titania is currently the subject of numerous studies due to the significance of this material for environmental catalysis. The photocatalytic effect makes it possible to perform the oxidative destruction of most organic pollutants and many pathogenic bacteria over titania at room temperature under UV exposure [1]. The attractiveness of titania-based photocatalysts is due to the effect of photocatalytic degradation of organic pollutants to elementary inorganic constituents. This opens up the prospect of using titania-based photocatalysts for sewage and air treatment, for creating self-cleaning glasses for building and automotive engineering, and for treating wall surfaces in hospitals and public buildings to reduce the level of bacterial contamination [2].

It is known that, when titania uptakes a photon with an energy greater than, or equal to, its bandgap width, an electron can be transferred from the valence band to the conduction band so as to generate an electron vacancy, referred to as a hole. Electrons and holes migrate to the surface of the catalyst where they participate in oxidation and reduction reactions with various adsorbate surface species. Holes can interact with water molecules bound to the catalyst surface to form a hydroxyl radical and a proton, or with hydroxo groups to form hydroxyl radicals OH<sup>•</sup>. Electrons can generate superoxide radical anion O<sup>2-</sup> in the course of reaction with oxygen. Hydroxyl and superoxide radical anions are presumably the main oxidizers in photocatalytic oxidation processes [3]. A specific feature of TiO<sub>2</sub> nanoparticles consists in the ability of reactive hydroxo groups to self-regeneration on their surfaces;

this appreciably enhances the sorption properties of the nanoparticles [4]. Thus, from the chemical standpoint, hydrated surface species on titania may be regarded as electron–hole recombination sites, and adsorbate oxygen molecules, as electron traps that suppress recombination [5]. Water molecules are natural surface modifiers for titania prepared by a hydrolytic sol–gel process. This sol–gel process affords excellent opportunities for manufacturing titania nanoparticles, whose surface charge and hydrate structure depend on the conditions under which the sol–gel process occurs [6].

The goal of this study was to elucidate how the charge and surface hydration of titania influence its photocatalytic activity. To attain this goal, we performed the sol–gel synthesis of titania nanopowders at various pH values and determined the activity of these nanopowders in photocatalytic destruction of organic dyes in aqueous suspensions under UV exposure with a constant oxygen concentration.

## EXPERIMENTAL

The chemicals used in the synthesis were titanium(IV) tetraisopropoxide (97%; from Aldrich), isopropanol (chemically pure grade), nitric acid (chemically pure grade), acetic acid (chemically pure grade), ammonia (chemically pure grade), and distilled water.

The titania synthesis protocol was as follows. Titanium tetraisopropoxide (10 g) was mixed with 100 mL isopropanol with a magnetic stirrer for 3 h at room temperature. Aqueous solutions having various pHs were prepared by adding nitric acid to adjust pH of 2,

acetic acid to adjust pH of 4, and ammonium hydroxide to obtain a solution with pH of 11. To a 500-mL portion of aqueous solutions, a mixture of isopropanol and titanium tetraisopropoxide (110 mL) was slowly added, followed by 24-h exposure under magnetic stirring (1000 rpm). The water/titanium isopropoxide molar ratio was 673 in all cases. The sols formed were separated by centrifugation, washed with water, and then dried in a drying cabinet at 110°C.

The powders prepared by the sol-gel route were characterized by IR spectroscopy (Avatar 360 FT-IR ESP) and thermal analysis (DSC 204 F1 Phoenix NETZSCH). An X-ray powder diffraction experiment was performed on a DRON-2 diffractometer. Coherent scattering lengths (crystallite sizes) were calculated by the Selyakov–Scherer relationship

$$D = K\lambda/\beta_{hkl} \cos\theta,$$

where  $K$  is particle form-factor (taken to be 0.94),  $\lambda$  is X-ray wavelength (0.15406 nm),  $\beta_{hkl}$  is peak width at half-height, and  $\theta$  is diffraction peak position. The precision of  $D$  calculations was 5%.

Specific surface areas and pore sizes were determined by low-temperature nitrogen adsorption/desorption (NOVA Series 1200e). Particle-size distributions and  $\zeta$  potentials were determined by dynamic light scattering on a Zetasizer Nano (Malvern Instruments) particle size and  $\zeta$  potential analyzer. The powders prepared according to the above-described protocol were dispersed in water having a neutral pH, and then measurements were carried out.

The photocatalytic activity of the prepared materials was tested in the destruction of organic dyes. The dyes used to be destructed were: Rodamine B (a dye having zwitterion structure), Methylene Blue (a cationic dye), and Anthraquinone AcidBlue (AcidBlue 80) (an anionic dye). We chose these dyes for their different charge types, in order to trace the effects of interactions of organic molecules having different charges

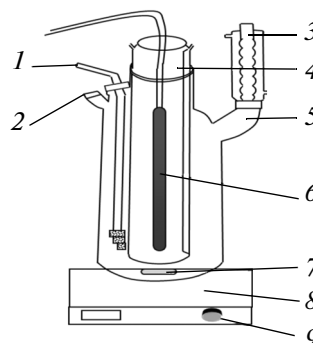


**Fig. 1.** Schematics of the setup used for carrying out photo-reactions: (1) oxygen supply, (2) sampling port, (3) cooler, (4) water-cooled silica jacket, (5) reaction flask, (6) UV lamp, (7) stirrer, (8) stirrer casing, and (9) rotation speed regulator.

with the surface of titania, and for their well-known photocatalytic degradation schemes [7–9].

A dye was photodegraded in a reactor which is schematically shown in Fig. 1. The UV radiation source was a high-pressure mercury lamp of 250 W in wattage with a radiation peak at 365 nm. The reaction vessel was a 800-mL cylindrical vessel, with a water-cooled jacket mounted inside and centered with the lamp. A magnetic stirrer was mounted on the reactor bottom. Air for flushing the reaction solution was admitted from the bottom to maintain a constant concentration of dissolved oxygen. The dye content of the solution was determined on a T70 + UV/Vis Spectrometer PG Instrument after an aliquot was sampled and centrifuged. The pre-irradiation of dye solutions for 1 h in the absence of photocatalysts showed that only insignificant (<2%) discoloration occurred during the pre-irradiation period.

The physicochemical characteristics of the powders prepared as described above are compiled in the table.

Physicochemical characteristics of titania powders prepared by a sol–gel process at various pHs

pH	$D_{cr}$ , nm	Particle size in suspension, nm	$\zeta$ , mV	Chemically bound water, %	$S_{sp}$ , m <sup>2</sup> /g (BET)	$d_{pore}$ , nm (BJH)	$V_p$ , cm <sup>3</sup> /g	Dye photodegradation rate constant, min <sup>-1</sup>	
2	6	650	+41	7	120	4	0.17	Rodamine B	0.26
								Methylene Blue	0.25
7	7	700	-14	10	310	3	0.26	Rodamine B	0.03
								Methylene Blue	0.05
								Acid Blue	0.06
11	10	350	-23	30	100	4	0.06	Rodamine B	0.02
								Acid Blue	0.0035

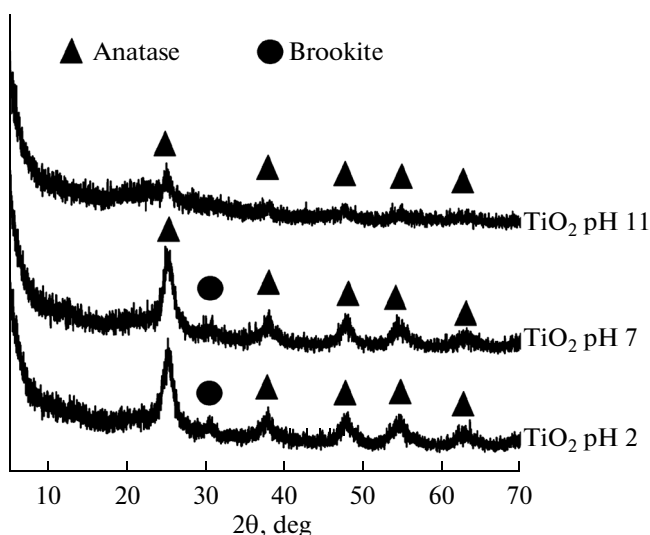


Fig. 2. X-ray diffraction patterns for TiO<sub>2</sub> hydrolysis products isolated from solutions at various pHs.

## RESULTS AND DISCUSSION

### *Effect of Sol–Gel Process Parameters on the Physicochemical Characteristics of Titania Powders*

Each of the numerous methods now used to prepare photocatalytically active titania-based nanomaterials [2] comprises a heat-treatment step intended to form the anatase (or anatase–rutile) crystal structure required for photocatalytic activity to appear. Heat treatment considerably alters the structure of initially formed particles and changes their degree of hydration and surface charge. So, such the studies give no opportunity to evaluate the photocatalytic activity of a material prepared directly by liquid-phase synthesis. The only exclusion is a hydrothermal method, which can help to prepare ultrafine photoactive TiO<sub>2</sub> polymorphs with tailored particle sizes [10].

The sol–gel process used in this study to prepare titania nanopowders involved the use of acid–base initiators of hydrolysis, high degree of molecular separation of hydrolysis products (attained due to the dilution of reagents), high water/alkoxide ratios, and high reagent mixing rates. As a result, all samples were built of crystallites which were amorphized to a considerable degree, likely due to the presence of a considerable amount of hydroxo species. X-ray powder diffraction showed anatase and brookite phases in the materials isolated from the colloid systems formed at pH of 2 or 7 (Fig. 2, Table 1). Cheng et al. [11] explained the effect of pH on the formation of titania polymorphs (in this case, brookite can appear as an intermediate between anatase and rutile phases).

Our results imply that TiO<sub>2</sub> crystallite sizes depend on pH maintained during the synthesis. Smaller crystallite sizes and higher crystallinities are typical of powders prepared in the presence of nitric acid. Materials prepared at pH ~ 7 had intermediate crystallite

sizes, and powders prepared at pH 11 typically had largest sizes of amorphized crystallites. We hold an opinion that this was due to the nitric acid induced acceleration of olation and oxolation during nanoparticle formation, which promoted the crystallization of low-hydrated products from a smaller number of structural units. Synthesis in an alkaline medium resulted in hydroxylated products with higher degrees of amorphism and larger crystallite sizes. These results agree with those published in [12].

More information about the hydration of materials was gained from the thermal analysis of powders. As probed by TGA (Fig. 3, Table), the highest TiO<sub>2</sub> yield was observed in solutions acidified with nitric acid, the lowest yield was in alkaline solutions, and the product yield from a neutral medium had intermediate values. Processing DTA curves as recommended by Avdin et al. [13], we found that the amount of bound water in titania increased as pH raised in the solution used for the synthesis. The powders had high specific surface areas as determined by low-temperature nitrogen adsorption/desorption (Fig. 4, Table). For the powders prepared at pH of 2, 7, and 11, the surface area was 120, 310, and 100 m<sup>2</sup>/g, respectively. All of the materials prepared typically had mesopores with sizes of 3–4 nm.

Photon correlation spectroscopy data for colloid structures formed by water-suspended particles and the ζ potentials of nanoparticles are shown as functions of synthesis parameters in Fig. 5 and in the table. Aggregate sizes (Fig. 5) have close values for TiO<sub>2</sub> samples prepared at different pHs, and this is important for the comparison of the photocatalytic activities of these samples in aqueous suspensions. The ζ potentials of TiO<sub>2</sub> particles prepared at pH of 2, 7, and 11 in aqueous suspensions are +41, –14, and –23 mV, respectively. The dependence of the nanoparticle surface charge on the synthesis parameters may be related to two factors. Firstly, synthesis in acidic medium results in the appearance of basic titania structural species formed by complexes [Ti(OH)<sub>2</sub>(H<sub>2</sub>O)<sub>4</sub>]<sup>2+</sup> (at pH 2), [Ti(OH)<sub>6</sub>]<sup>2–</sup> (at pH 7), and [Ti(OH)<sub>7</sub>]<sup>3–</sup> (at pH 9) [5]. Secondly, the formation of TiO<sub>2</sub> nanoparticles in a sol–gel process carried out at some pH is accompanied with chemisorption, which determines the surface charge of nanoparticles [14]:

for pH < 3.5: TiO<sub>2</sub> + nH<sup>+</sup> ↔ TiO<sub>2</sub>H<sub>n</sub><sup>n+</sup> (plus counterions); and

for pH > 3.5: TiO<sub>2</sub> + nOH<sup>–</sup> ↔ TiO<sub>2</sub>(OH)<sub>n</sub><sup>n–</sup> (plus counterions).

The sum of the above contributions determines the total value of the ζ potential of nanoparticles. The sign of the ζ potential for nanoparticles prepared under different conditions is retained after the nanoparticles are washed and then dried for several weeks. Interestingly, the behavior of the ζ potential of TiO<sub>2</sub> nanoparticles dispersed in neutral-pH water as a function of synthe-

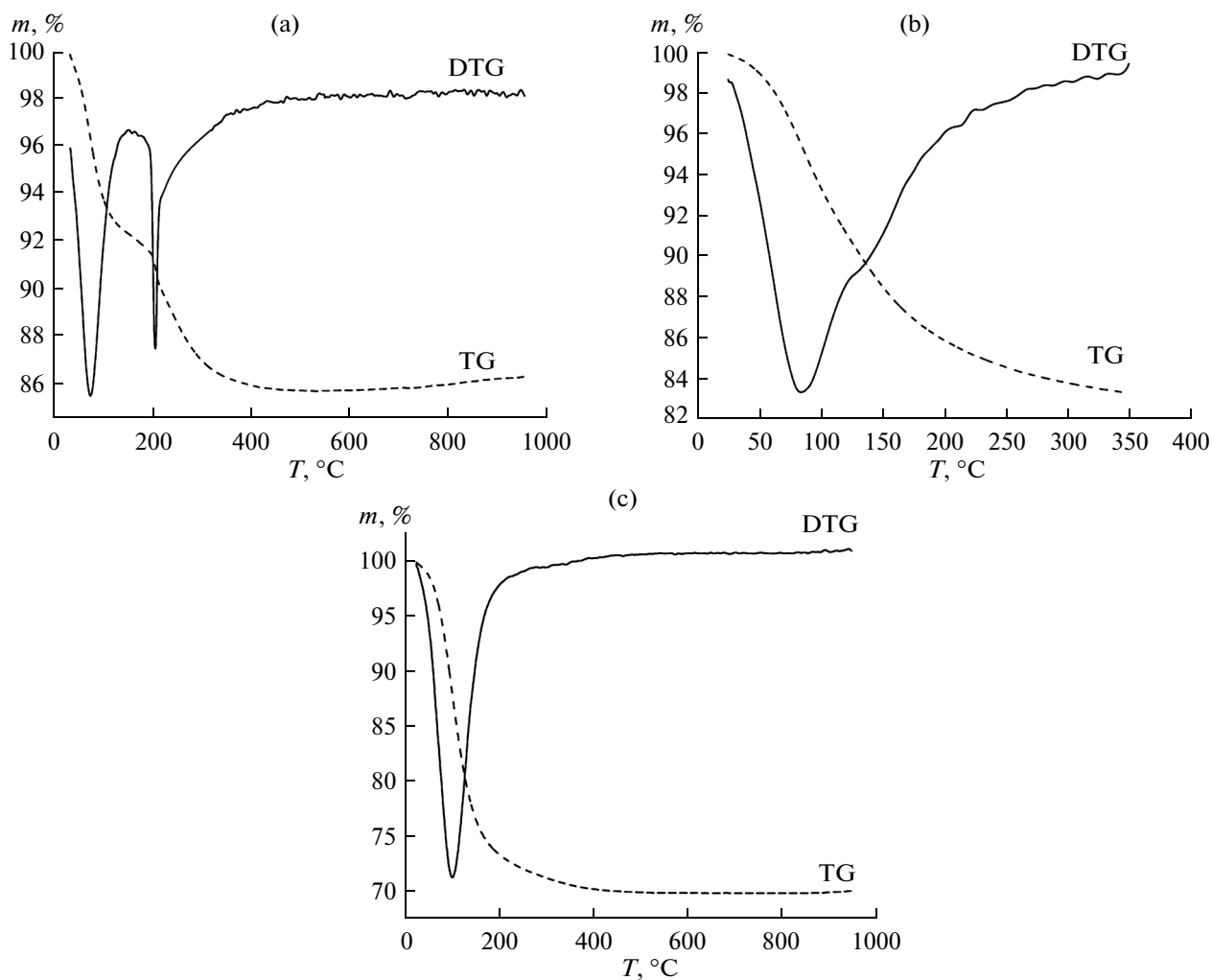


**Fig. 3.** Thermoanalytical data for powders of  $\text{TiO}_2$  hydrolysis products isolated from solutions at various pHs: (a) pH 2, (b) pH 7, and (c) pH 11 (heating to  $1000^\circ\text{C}$  at a rate of  $5\text{ K/min}$ ).

sis pH is like the behavior of the  $\zeta$  potential of titania nanoparticles as a function of aqueous pH [15].

#### *Photocatalytic Properties of Materials Prepared*

Photodegradation rate curves for model pollutants under UV exposure are shown in Fig. 6. An inspection of dye degradation rates in the reactor implies that titania samples prepared at various pHs have high photocatalytic activities. The photodegradation rate constants obtained in the Langmuir–Hinshelwood model are listed in the table. The rate constants are not in direct relation to the surface areas of photocatalysts. Meanwhile, noteworthy are the different contributions of adsorption and photocatalytic processes proper to the photocatalytic destruction of dyes over  $\text{TiO}_2$  depending on the degree of hydration and the surface charge. We failed to determine the photodestruction kinetic characteristics for Methylene Blue over  $\text{TiO}_2$  samples prepared at pH of 11 and for

Anthraquinone AcidBlue over  $\text{TiO}_2$  samples prepared at pH of 2. Our failure was due to the fast and quantitative irreversible adsorption of these dyes on the corresponding photocatalysts at the dye/titania ratios studied. The complete adsorption of Methylene Blue and Anthraquinone AcidBlue on  $\text{TiO}_2$  was observed in few minutes; the dye was not detected spectrophotometrically in solution after this period of time.

Irradiation of suspensions of titania having adsorbate dyes resulted in the degradation of the dyes over the catalyst surface within 15–30 min. Our attempts to spectrophotometrically measure photodestruction kinetics failed. In this case, we observed the complete and irreversible adsorption of dyes on the surface of  $\text{TiO}_2$  as a result of electrostatic interactions. In other cases, the dyes under study were adsorbed on  $\text{TiO}_2$  slowly (equilibrium was acquired no sooner than in 1 h). For example, it was shown spectrophotometrically that steady-state adsorption of Rhodamine B on the titania surface was acquired after 1-h exposure in the dark

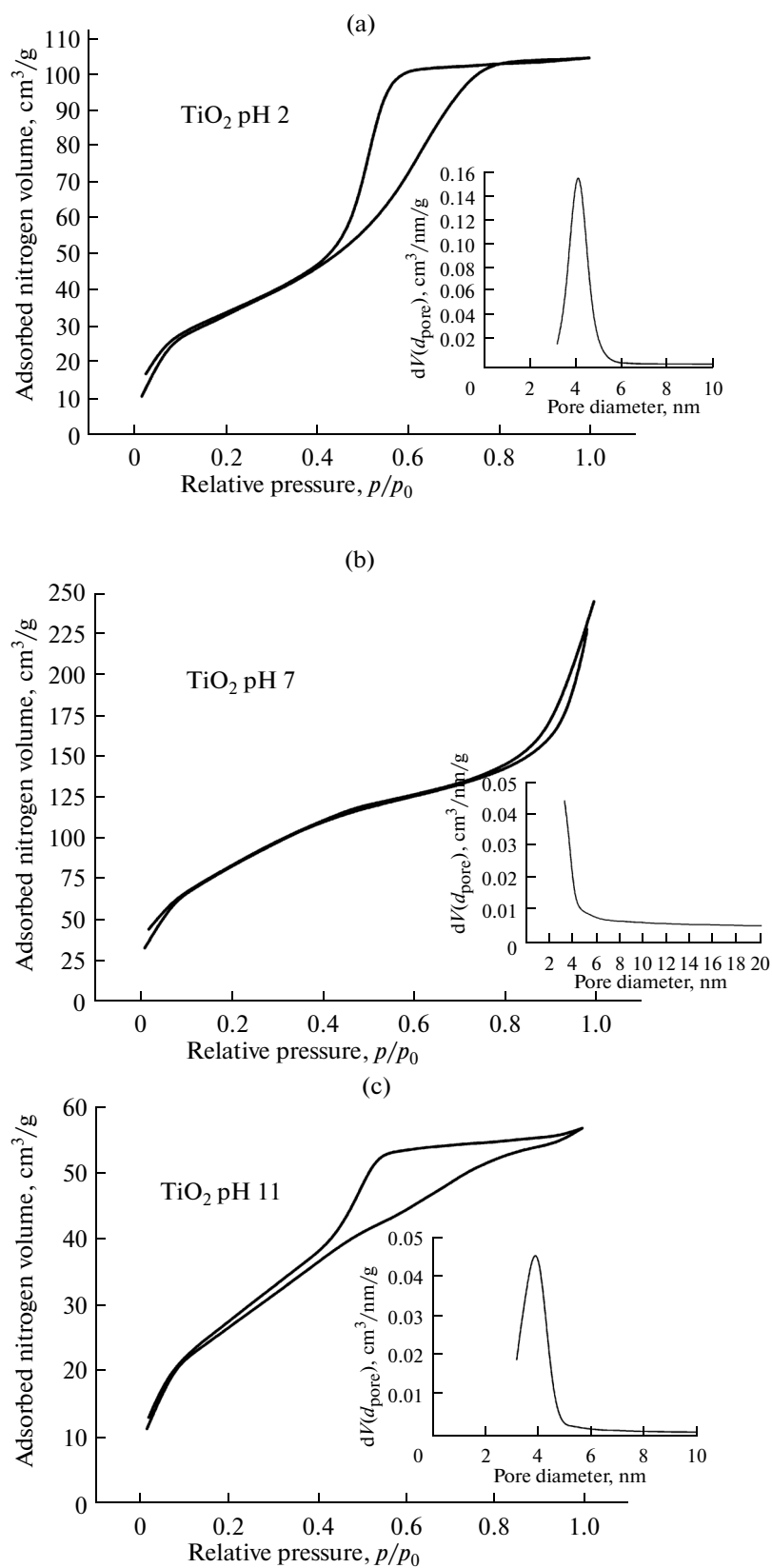
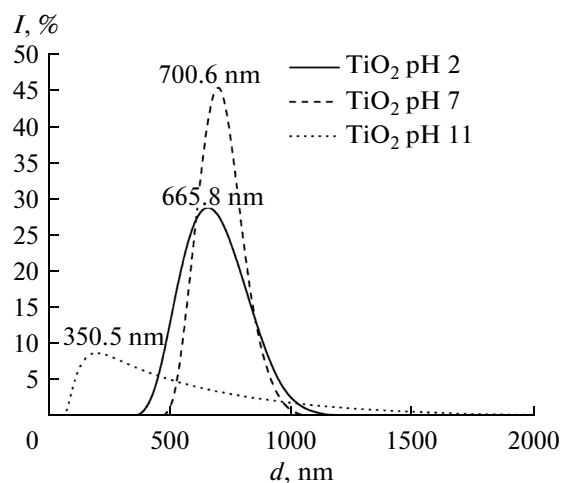


Fig. 4. Low-temperature nitrogen adsorption/desorption by  $\text{TiO}_2$  hydrolysis products isolated from solutions at various pHs.



**Fig. 5.** Particle-size distribution for powdery  $\text{TiO}_2$  hydrolysis products isolated from solutions at various pHs.

under stirring and amounted to 84% (in percent of the initial dye concentration  $C = 0.00215$  g/L) for the powders prepared at pH of 2, 95% for those prepared at pH of 7, and 74% at pH of 11. In this case, the adsorption value correlated with the surface area of the powder.

The photocatalytic activity for all types of dyes studied decreases in the order of our prepared photocatalysts as follows:  $\text{TiO}_2$  (pH 2) >  $\text{TiO}_2$  (pH 7) >  $\text{TiO}_2$  (pH 11). The highest activity is observed for titania powders prepared in the presence of nitric acid. (Patrick and Dietmar [7] also found that titania samples prepared by a hydrothermal route in the presence of nitric acid had higher photocatalytic activities than samples isolated from acid-free solutions.)

Analysis of the data gained in this study shows that the photocatalytic activity decreases in the series of the materials studied in response to an increase in the degree of surface hydroxylation, the total content of chemically bound water, and the negative value of  $\zeta$

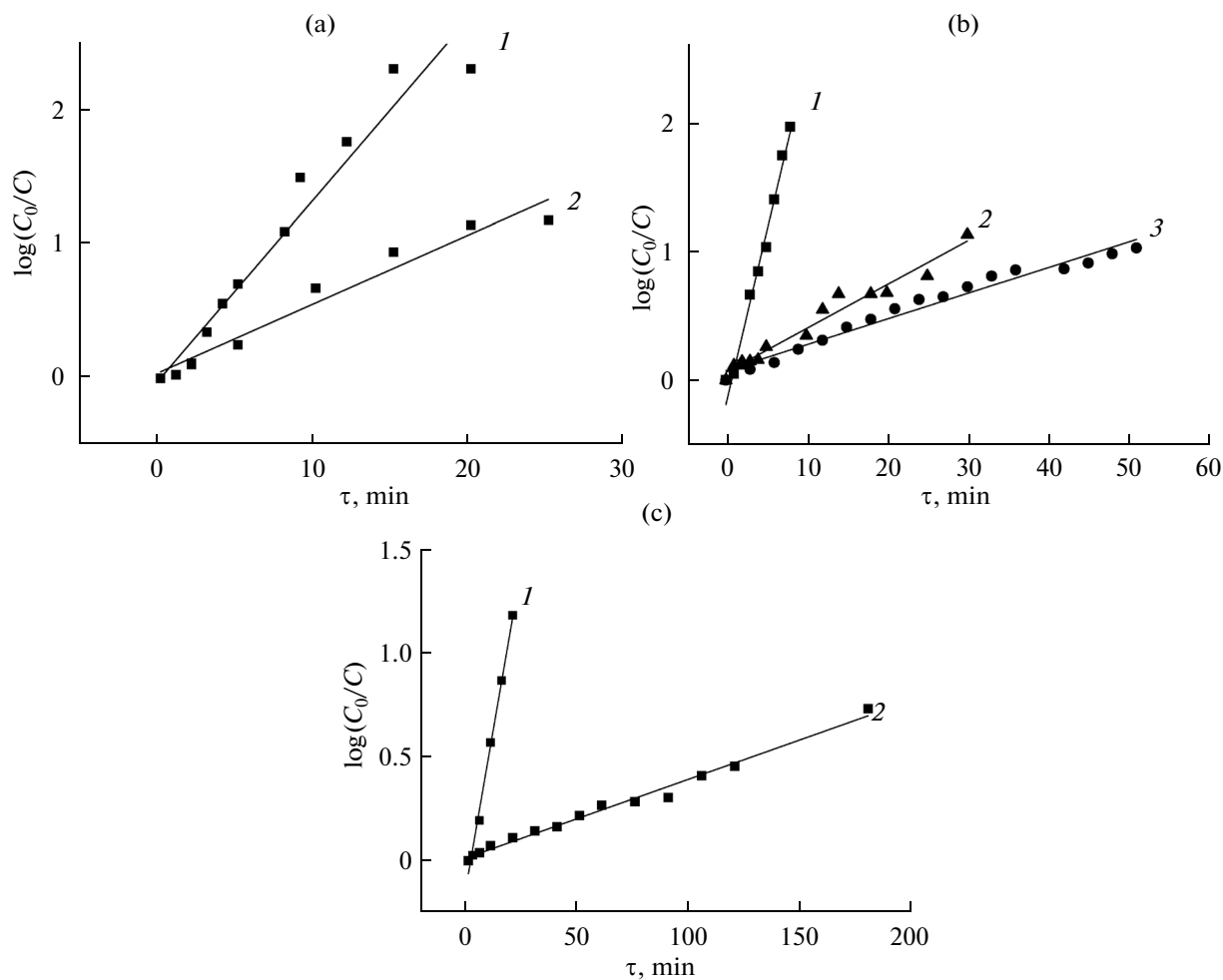
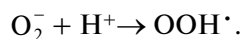


**Fig. 6.** Organic dye photodegradation rate curves in aqueous suspensions of powdery  $\text{TiO}_2$  hydrolysis products isolated from solutions at various pHs. (a) Methylene Blue: (1) pH 2 and (2) pH 7; (b) Rodamine B: (1) pH 2, (2) pH 7, and (3) pH 11; and (c) Anthraquinone AcidBlue (1) pH 7 and (2) pH 11, under UV exposure.

potential. This occurs despite the greater surface areas of hydroxylated products prepared at pH 7 and 11 compared to the surface area of TiO<sub>2</sub> prepared in the presence of nitric acid. We believe that the considerable gain in photocatalytic activity of titania prepared at pH of 2 is due to the greater mobility of a proton that is not bonded directly to the surface of TiO<sub>2</sub> and is involved in the structure of hydroxonium ions, which interact with the surface through hydrogen bonds, compared to the hydroxide groups in the structure of hydroxylated titania species. High hydroxonium ion concentrations create beneficial conditions for OOH<sup>•</sup> radicals to appear as a result of the formation of a protonated superoxide ion species on the TiO<sub>2</sub> surface:



Obviously, the high photocatalytic activity of titania prepared by sol–gel synthesis in acid solutions, is due to high concentrations of hydroperoxide radicals on the catalyst surface.

In summary, we have studied the effects of parameters of sol–gel synthesis performed with a high degree of molecular separation upon the dilution of reagents, high water/alkoxide ratio, and high reagent mixing rates in aqueous solution at pH of 2, 7, and 11. We have found that these synthesis parameters can provide the production of nanocrystalline anatase powders or anatase powders admixed with brookite, having specific surface areas higher than 100 m<sup>2</sup>/g and containing mesopores with sizes of 3–4 nm.

The ζ potentials of titania particles prepared at pH of 2, 7, and 11 in aqueous suspensions are +41, –14, and –23 mV, respectively. The nanoparticles prepared under various synthesis parameters retain the sign of their ζ potential after being washed and dried for few weeks.

The photocatalysts prepared are arranged in the following order of decreasing Rodamine B, Methylene Blue, and Anthraquinone AcidBlue photodestruction rates under UV exposure: TiO<sub>2</sub> (pH 2) > TiO<sub>2</sub> (pH 7) > TiO<sub>2</sub> (pH 11). The effects of the surface area, ζ potential, and the charge type of dye and the surface hydration specifics of titania nanoparticles on the dye degradation rates have been detailed.

## ACKNOWLEDGMENTS

The authors are grateful to the Collected Research Facility Center “Upper Volga Regional Center for Physicochemical Research.”

This study was performed in the frame of the Government Assignment of the Ministry of Education and Science of Russia (no. 11.801.2014/K) and was in part supported by the Russian Foundation for Basic Research (project no. 14-03-00502).

## REFERENCES

1. A. Fujishima, K. Hashimoto, and T. Watanabe, *TiO<sub>2</sub>: Photocatalysis, Fundamentals and Applications* (BKC, Tokyo, 1999).
2. K. Nakata and A. Fujishima, *J. Photochem. Photobiol. C: Photochem. Rev.* **13**, 169 (2012).
3. A. L. Linsebigler, G. Lu, J. T. Yates, Jr., et al., *Chem. Rev.* **95**, 735 (1995).
4. L. N. Obolenskaya, N. A. Dulina, E. V. Savinkina, and G. M. Kuz'micheva, *Inorg. Mater.* **49**, 609 (2013).
5. P. Salvador, *J. Phys. Chem.* **111**, 17038 (2007).
6. W. Zhang, S. Chen, S. Yu, et al., *J. Cryst. Growth* **308**, 122 (2007).
7. W. Patrick and S. Dietmar, *J. Photochem. Photobiol., A* **185**, 19 (2007).
8. A. Houas, H. Lachheb, M. Ksibi, et al., *Appl. Catal. B: Env.* **31**, 145 (2001).
9. Y. Su, L. Deng, N. Zhang, et al., *React. Kinet. Catal. Lett.* **98**, 227 (2009).
10. V. K. Ivanov, V. D. Maksimov, A. S. Shaporev, et al., *Russ. J. Inorg. Chem.* **55**, 184 (2010).
11. H. Cheng, J. Ma, Z. Zhao, and L. Qi, *Chem. Mater.* **7**, 663 (1995).
12. S. Mahshid, M. Askari, M. Ghamsari, et al., *J. Mater. Proc. Technol.* **189**, 296 (2007).
13. V. V. Avdin, A. A. Lyar', and A. V. Batist, *Vestn. Yuzhno-Ural. Gos. Univ., Ser. Math., Mekh., Fiz., No. 7*, 211 (2006).
14. D. Bahnemann, A. Henglein, and L. Spanhe, *Faraday Discuss. Chem. Soc.* **78**, 151 (1984).
15. K. Suttiponparnit, J. Jiang, M. Sahu, et al., *Nanoscale Res. Lett.* **6**, 1 (2011).

*Translated by O. Fedorova*